Supporting Information for

Crystallographic snapshots of the Zika virus NS3 helicase help visualize the reactant water replenishment

Junnan Fang[1,#], Xuping Jing[2,3,#], Guoliang Lu[2], Yi Xu[1, 2]*, Peng Gong[1, 2]*

1. The Joint Center of Translational Precision Medicine: Guangzhou Institute of Pediatrics, Guangzhou Women and Children's Medical Center, Guangzhou, Guangdong, 510623, China; Wuhan Institute of Virology, Chinese Academy of Sciences, Wuhan, Hubei, 430071, China;

2. Key Laboratory of Special Pathogens and Biosafety, Wuhan Institute of Virology, Chinese Academy of Sciences, Wuhan, Hubei, 430071, China;

3. University of Chinese Academy of Sciences, Beijing, 100049, China.

# J.F. and X.J. contributed equally to this work.

* Correspondence: gongpeng@wh.iov.cn (P.G.), xuyi70@163.com (Y.X.)

Pages: S1-S6

Figures S1-S2; Movie Legend S1

Supplymental Figures and Legends

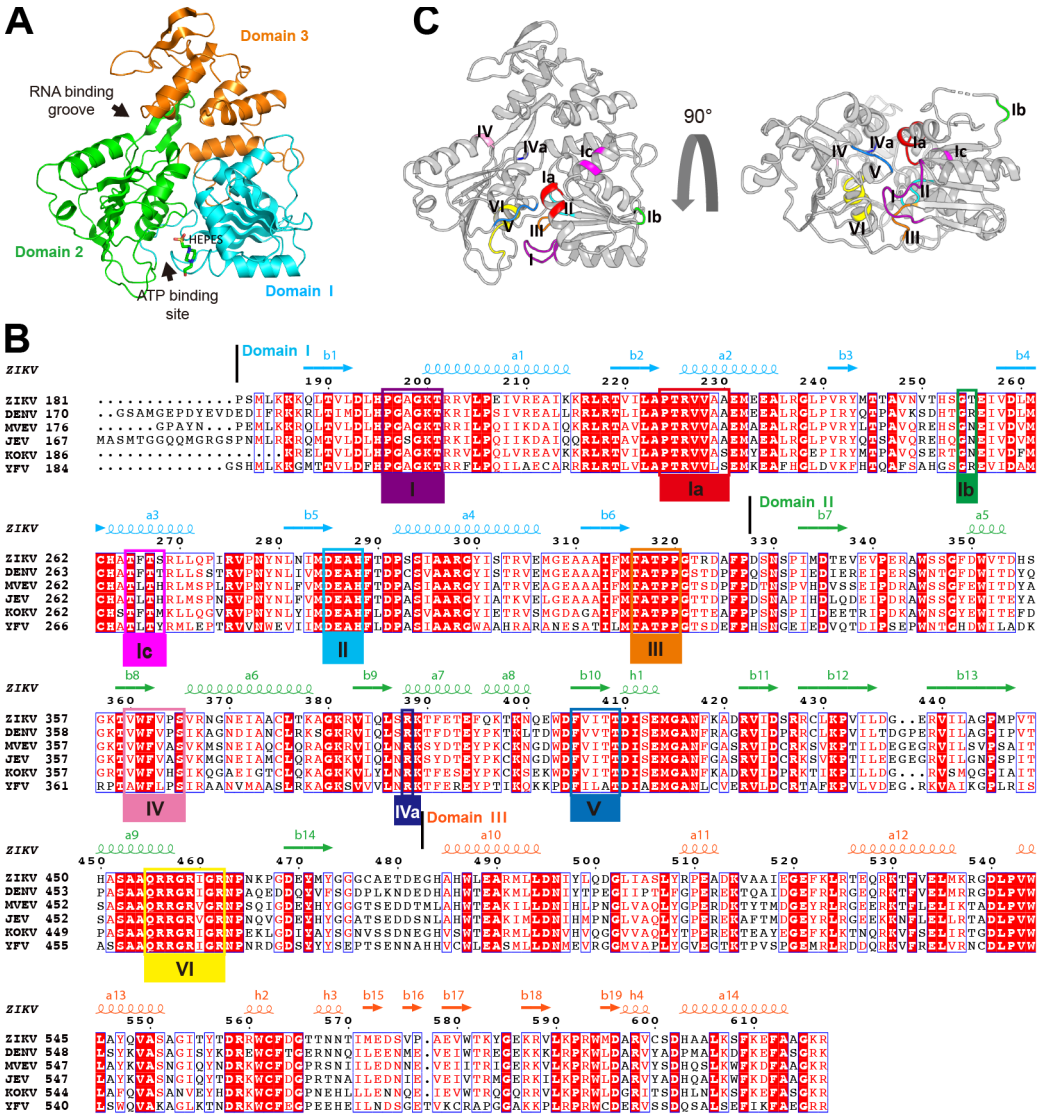

Figure S1. The three-dimensional structure of ZIKV NS3_Hel (apo) and its alignment with representative flavivirus NS3_Hel sequences. A) Ribbon diagram of ZIKV NS3_Hel (apo) with Domain 1 in green, Domain 2 in cyan, and Domain 3 in orange. The HEPES molecule bound in the ATP binding site are shown in sticks. (B) Sequence alignment of representative flavivirus NS3 helicases. The sequences of Dengue virus (DENV, UniProt entry Q2YHF0), Murray valley encephalitis virus (MVEV, UniProt entry P05769), Japanese encephalitis virus (JEV, UniProt entry P27395), Kokobera virus (KOKV, UniProt entry Q32ZD5), and Yellow Fever virus (YFV, UniProt entry P03314) were obtained from UniProTKB. Secondary structure element symbols (spring: helix; arrow: β-strand) of ZIKV NS3_Hel are displayed

above the sequence alignment. The conserved ATPase motifs are marked in purple (I), red (Ia), green (Ib), magenta (Ic), cyan (II), orange (III), pink (IV), dark blue (IVa), blue (V), and yellow (VI). (C) ATPase motifs in ZIKV NS3_Hel apo crystal structure. The coloring scheme matches that of the colored bars displayed below the sequence alignments in panel B.

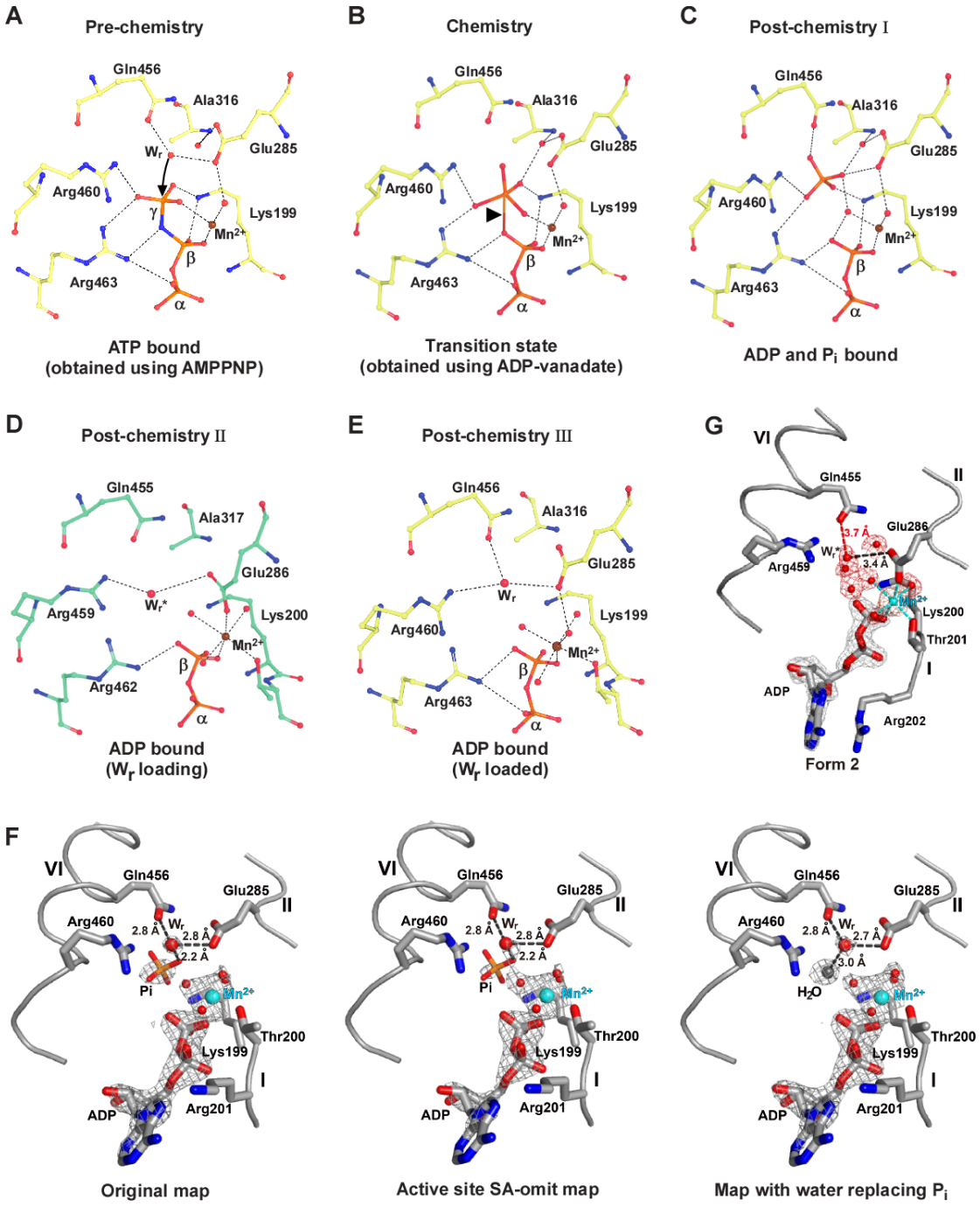

Figure S2. The catalytic mechanism for ATP hydrolysis by flavivirus NS3_Hel illustrated by five representative states. A) The first state obtained using an ATP analog AMPPNP represents the ATP bound pre-chemistry state. The reactant water is hydrogen-bonded by the side chain atoms of Glu285 (motif II) and Gln456 (motif VI), ready for an in-line nucleophilic attack of the γ-phosphate (indicated by the arrow). B) The second state obtained using ADP-vanadate mimics the transition state. The solid triangle indicates where the bond breaks. C) The third state represents a product complex with both ADP and P_i bound. The reactant water in the reported model is not

shown due to the reason of its close contact with one of the P_i oxygen atoms. Although we propose that this structure may represent an ADP-Mn complex, it is still used in this scheme to represent an ADP-P_i-Mn complex. D) The fourth state represents a product complex with ADP bound and the reactant water in a loading state. E) The fifth state represents a product complex with ADP bound and the reactant water already loaded. Structures shown in panels A, B, C, and E were adapted from the DENV work (PDB entries 2JLV, 2JLX, 2JLY, and 2JLZ, respectively) (1) and the structure in panel D is the form 2 ZIKV NS3_Hel-ADP-Mn (PDB entry 6ADY) in this work. F) An analysis of the previously reported structural data of the DENV ADP-Pi-Mn model (PDB entry 2JLY). Left: original model with original $2F_o$-F_c electron density map overlaid. Middle: original model with a 3,500 K simulated-annealing (SA) active site omit map (i.e. all non-protein components in the active site were omitted for calculation) overlaid. The density around the modeled Pi is apparently weaker than that in the original map and is comparable to that of the nearby water molecules. Right: The re-refined model and $2F_o$-F_c electron density map obtained using a modified input model with a water molecule replacing the P_i. In the re-refined model, the B-factor of the P_i-replacing water molecule is about 25 $Å^2$, comparable to that of the neighboring water molecules, and is apparently lower than that of the P_i in the original model (about 47 $Å^2$). Mn^{2+} coordination interactions, the hydrogen bonds formed between the W_r and residues Gln456 and Glu285, and the close contact between the P_i and the reactant water are shown as dashed lines. All maps are contoured at 1.8 σ. G) The ZIKV NS3_Hel-ADP-Mn form 2 structure overlaid with a 3,500 K SA active site omit map calculated by the PHENIX software suite (2). This analysis complements the data shown in Figure 1E (maps calculated by CNS (3)), and together provides a validation of the observed position of the reactant water in a loading state.

Supplymental Movie Legend

Movie S1. An animation helps visualize the reactant water loading in ZIKV NS3_Hel. The animation starts with the ZIKV NS3_Hel-ADP-Mn form 2 complex (PDB entry 6ADY) and ends with the ZIKV NS3_Hel-ADP-Mn form 1 complex (PDB entry 6ADX). The Mn^{2+} is shown as a cyan sphere; the reactant water is shown as a big red sphere; three Mn^{2+} coordinating water molecules are shown as small red spheres. Key side chains involved in ADP binding, Mn^{2+} coordination and reactant water interactions are shown as sticks. Mn^{2+} coordination interactions are shown as cyan dashed lines. The distances between the reactant water and key residues Glu286/ Gln455 are shown with red dashed lines.

Supplymental References

1. Luo, D., Xu, T., Watson, R.P., Scherer-Becker, D., Sampath, A., Jahnke, W., Yeong, S.S., Wang, C.H., Lim, S.P., Strongin, A. *et al.* (2008) Insights into RNA unwinding and ATP hydrolysis by the flavivirus NS3 protein. *The EMBO journal*, **27**, 3209-3219.
2. Adams, P.D., Grosse-Kunstleve, R.W., Hung, L.W., Ioerger, T.R., McCoy, A.J., Moriarty, N.W., Read, R.J., Sacchettini, J.C., Sauter, N.K. and Terwilliger, T.C. (2002) PHENIX: building new software for automated crystallographic structure determination. *Acta crystallographica. Section D, Biological crystallography*, **58**, 1948-1954.
3. Brunger, A.T., Adams, P.D., Clore, G.M., DeLano, W.L., Gros, P., Grosse-Kunstleve, R.W., Jiang, J.S., Kuszewski, J., Nilges, M., Pannu, N.S. *et al.* (1998) Crystallography & NMR system: A new software suite for macromolecular structure determination. *Acta crystallographica. Section D, Biological crystallography*, **54**, 905-921.